

IV. RESULTS

Cytokines are integral components of the intercellular communication network. They are required to mount and control immune responses. Their quantification is therefore regarded as an important way to study the specific functions of immune cells. Interferon gamma (IFN γ) is a T-cell-derived cytokine with broad macrophage-activating effects, and known to play a critical role in cellular immunity. In the same way, interleukin 4 (IL-4) is involved in the humoral response and possibly in the development of some atopic diseases since it triggers the T helper 2 response (Th2) and on its own IgE development. Therefore, IL-4 is a candidate gene for disease association studies and gene mapping. Here, its monitoring would be useful for studying the balance of the immune response.

4.1. Cloning of IFN γ and IL-4

In order to characterize the T helper 1 (Th1) responses of domestic horse (*Equus caballus*) as a model species, its hallmark cytokine gene, IFN γ , was cloned and compared to IFN γ sequences of zoo equids such as; Somali wild ass (*Equus africanus somalicus*), Hartmann's mountain zebra (*Equus zebra hartmannae*) and Grevy's zebra (*Equus grevyi*). In addition, IFN γ of other mammalian species namely Indian one-horned rhinoceros (*Rhinoceros unicornis*), Asian elephant (*Elephas maximus*), Nubian giraffe (*Giraffa camelopardalis*), European bison (*Bison bonasus*) and African buffalo (*Syncerus caffer*) were included and compared to sequences available *via* GenBank. The cDNAs encoding for IFN γ were amplified by reverse transcription polymerase chain reaction (RT-PCR) using primers delineated from reported sequences of equine, bovine, mice and human IFN γ sequences.

In parallel, cloning and sequencing of IL-4 as hallmark cytokine gene of Th2 responses was performed from horse and most previously mentioned zoo animals (with the exception of Grevy's zebra) by the same method based on published IL-4 GenBank sequences.

4.1.1 IFN γ

The cDNAs encoding for IFN γ were amplified using two pairs of primers (outer and inner) primer pairs, with specific wobble positions to allow their use for all species (3.2.3.3). The outer primer pair was designed to flank an area of the IFN γ gene outside the ORF while the inner primer pair spanned across the entire ORF.

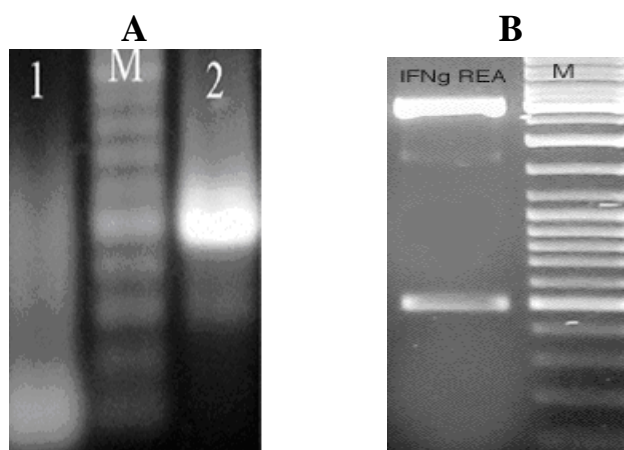


Fig. 1 IFN γ PCR (first and nested) and restriction enzyme endonuclease analysis.

Fig. 1-A Agarose gel electrophoresis of PCR products amplified by IFN γ degenerated delineated outer and inner primers sets. cDNA was transcribed using outer reverse primer. Sequences amplified using designed IFN γ outer primers (1) resulted in multiple unspecific products. 4 μ l of such PCR were taken in a second (nested) PCR using the IFN γ inner primer pair (2). This nested PCR gave the specific target product size (approximately 501bp).

Fig. 1-B Restriction enzyme endonuclease analysis EcoR I was used to determine successful cloning of IFN γ cDNA into pGEM-T Easy vector (here elephant IFN γ). Lane 1 is the elephant IFN γ (501 bp). M is the DNA ladder marker (100bp).

As is evident in figure 1-A, IFN γ outer primers were not able to amplify one specific DNA. The nested PCR, however, detected the target DNA specifically. In addition, the inner pair worked specific over a broad variety of mammalian species, but was on its own not sufficient to amplify the sequences (data not shown).

Cloning of IFN γ nested PCR product of different species was carried out using pGEM-T Easy Vector (3.2.3.7). Restriction enzyme endonuclease analysis (REA) was performed (Fig. 1-B) in order to confirm cloning prior to sequencing with plasmid-specific upstream and downstream primers (3.2.3.8).

Cloning and sequencing of IFN γ revealed that the ORFs of all examined animal species were found to be 501 bp in length (Fig. 2), encoding for 166 amino acids (Fig. 3).

Phylogenetic profile of these sequences revealed high homology among perissodactyls with few differences between equids and Indian rhinoceros. Close relationship was evident between IFN γ of artiodactyls with highest homology among bovids. A substantial degree of homology was also found between perissodactyls and artiodactyls. Human IFN γ is closer related to both perissodactyls and artiodactyls than to mice (Fig. 4 and table 1).

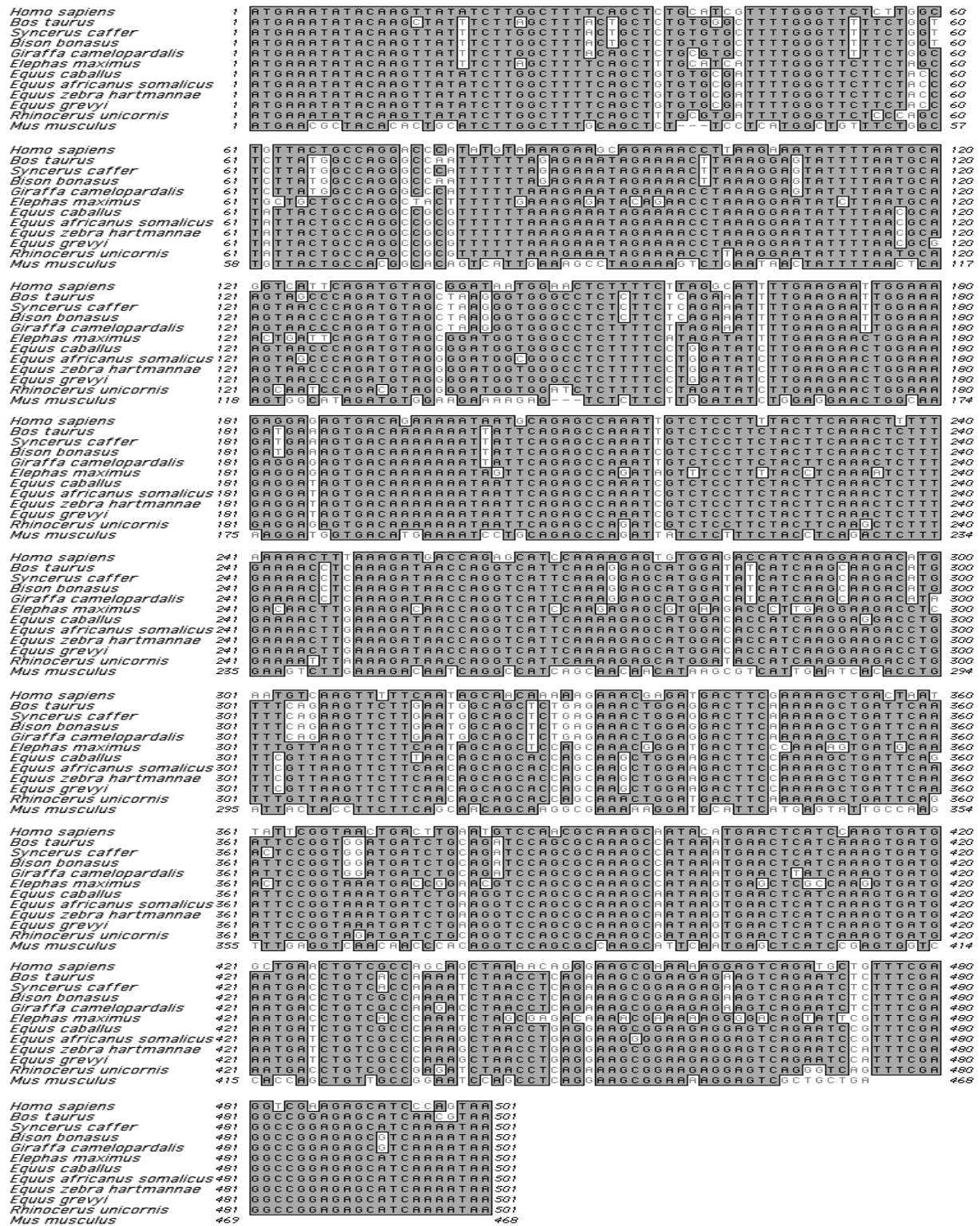


Fig. 2 Nucleic acid alignment of IFN γ sequences.

IFN γ ORF sequences from African buffalo (*Syncerus caffer*), European bison (*Bison bonasus*), Nubian giraffe (*Giraffa camelopardalis*), Asian elephant (*Elephas maximus*), horse (*Equus caballus*), Somali wild ass (*Equus africanus somalicus*), Hartmann's mountain zebra (*Equus zebra hartmannae*), Grevy's zebra (*Equus grevyi*) and Indian one-horned rhinoceros (*Rhinoceros unicornis*) were aligned with reported IFN γ sequences of human (*Homo sapiens*) (GenBank: M37265), bovine (*Bos taurus*) (M29867) and mice (*Mus musculus*) (K00083). All species IFN γ ORFs (except mice) are of the same size (501 bp). Sequence differences between species are white coloured while identities are dark grey in colour. The first 29 and last 26 bases of cloned sequences are primer derived.



Fig. 3 IFN γ amino acid alignment.

The complete ORFs sequences of African buffalo, European bison, Nubian giraffe, Asian elephant, horse, Somali wild ass, Hartmann’s mountain zebra, Grevy’s zebra and Indian one-horned rhinoceros were compared to reported IFN γ sequences of human, cattle and mouse. Protein identities are dark grey coloured while different proteins are white.

Phylogenetic analysis of IFN γ protein sequences provided a visual account of how closely related species are to one another (Fig. 4).

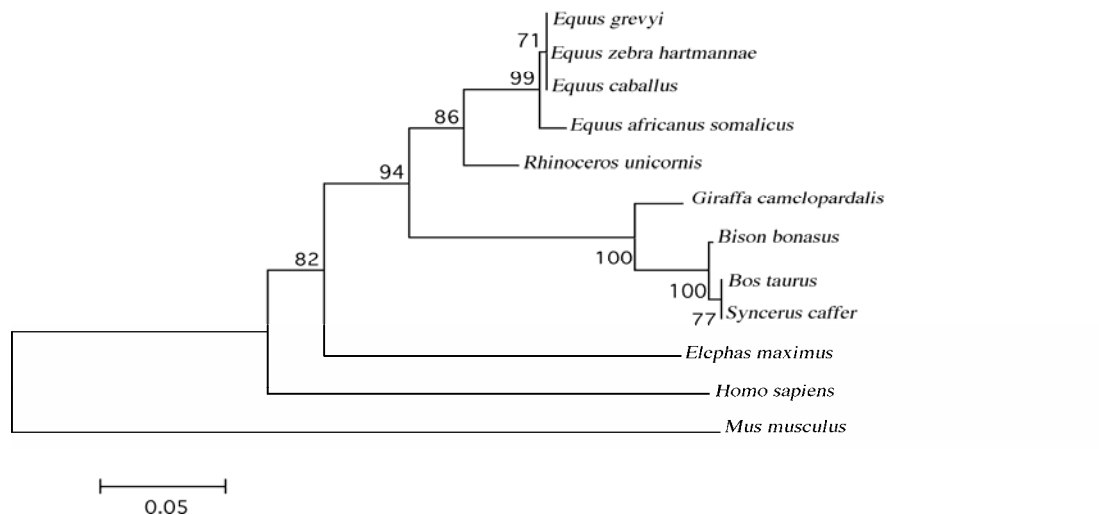


Fig. 4 Phylogenetic relationships between animal species based on comparison of IFN γ aa sequences.

The deduced amino acid sequences alignment was carried out using MEGA3 software package and Neighbour joining tree with Bootstrap (1000 replicates) analysis and gaps distributed proportionally to analyse phylogenetic relation of IFN γ protein sequences. Horizontal branches were drawn to scale. Bar, 0.05 aa substitutions per site. Mouse IFN γ was used as an out-group. The perissodactyls clustered together and were divided into *Equidae* and the Indian rhinoceros as a sole analysed member of the family *Rhinocerotidae*. Alike, the artiodactyls grouped together with two major branches the first containing only the Nubian giraffe and the second all members of family *Bovidae*. The Asian elephant remained unrelated to these groups.

The IFN γ amino acid sequences were also analyzed pairwise for homology (table 1). Significant protein homologies were detected among perissodactyls (horse, Somali wild ass, two zebra species and Indian rhinoceros) and artiodactyls (African buffalo and European bison and Nubian giraffe). While the homology between humans and any of the animal species analysed were 72-79%, mice displayed only 54-57% homology. The Asian elephant was slightly closer related to perissodactyls, which may be of help to detect cross-reacting tools for immunology.

Table (1) IFN γ proteins pairwise analysis:

| Human | Bovine | African buffalo | European bison | Nubian giraffe | Asian elephant | Horse | Somali wild ass | Hartmann's zebra | Grevy's zebra | Indian rhinoceros | Mouse | Species |
|-----------|----------|-----------------|----------------|----------------|----------------|-----------|-----------------|------------------|---------------|-------------------|-----------|----------------------------------|
| 100 (100) | 72 (61) | 75 (62) | 74 (61) | 76 (64) | 75 (65) | 78 (68) | 77 (68) | 78 (68) | 78 (68) | 79 (69) | 54 (38) | <i>Homo sapiens</i> |
| | 100(100) | 97 (97) | 98 (98) | 95 (93) | 76 (65) | 85 (78) | 85 (78) | 85 (78) | 85 (78) | 85 (78) | 55 (41) | <i>Bos taurus</i> |
| | | 100 (100) | 98 (98) | 97 (95) | 78 (67) | 86 (79) | 84 (77) | 86 (79) | 86 (79) | 86 (79) | 56 (41) | <i>Syncerus caffer</i> |
| | | | 100 (100) | 97 (95) | 77 (66) | 86 (79) | 85 (78) | 86 (79) | 86 (79) | 87 (80) | 56 (41) | <i>Bison bonasus</i> |
| | | | | 100 (100) | 78 (67) | 87 (81) | 86 (80) | 87 (81) | 87 (81) | 87 (82) | 56 (41) | <i>Giraffa camelopardalis</i> |
| | | | | | 100 (100) | 84 (75) | 83 (74) | 84 (75) | 84 (75) | 83 (75) | 55 (38) | <i>Elephas maximus</i> |
| | | | | | | 100 (100) | 98 (98) | 100 (100) | 100 (100) | 96 (92) | 57 (43) | <i>Equus caballus</i> |
| | | | | | | | 100 (100) | 98 (98) | 98 (98) | 95 (91) | 56 (42) | <i>Equus africanus somalicus</i> |
| | | | | | | | | 100 (100) | 100 (100) | 96 (92) | 57 (43) | <i>Equus zebra hartmannae</i> |
| | | | | | | | | | 100 (100) | 96 (92) | 57 (43) | <i>Equus grevyi</i> |
| | | | | | | | | | | 100 (100) | 56 (43) | <i>Rhinoceros unicornis</i> |
| | | | | | | | | | | | 100 (100) | <i>Mus musculus</i> |

Legend to table (1)

Sequences revealed an extended homology (identity and similarity) among IFN γ amino acids of perissodactyls (green) and artiodactyls (blue) each. Mice share only little degree of homology with any of the analysed species, while humans were at least 72% homologous.

Numbers provided are percentages of homology as calculated by pairwise amino acid sequence alignment using MacVector software package (the numbers in brackets are identical aa in %).

4.1.2 IL-4

For cloning of IL-4 of different species, the analogous approach as for IFN γ was successfully used (Fig. 5-A). However during cloning and further analysis it became evident that the size of IL-4 of the different species was not identical as best visualized at nested PCR products (Fig. 5-B).

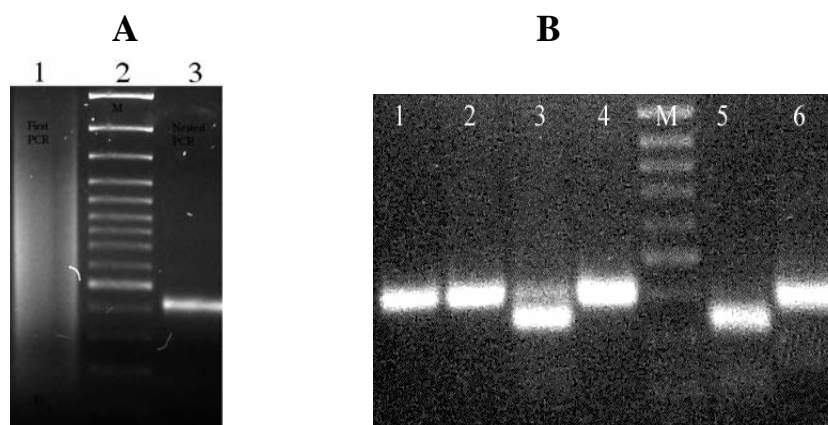


Fig. 5 Agarose gel electrophoresis of IL-4 PCR products.

Fig. 5-A Agarose gel electrophoresis of IL-4 PCR products amplified by degenerated delineated outer and inner primers sets. cDNA was transcribed using outer reverse primer. Sequences were amplified using IL-4 outer primers (1) resulted in many unspecific products. 4 μ l of such PCR were taken in a second (nested) PCR using IL-4 inner primer pair (3). This nested PCR provided the specific target product size (414 bp for horse IL-4). DNA ladder marker lane (2).

Fig. 5-B Agarose gel electrophoresis of IL-4 nested PCR products of different animal species. Lane (1) is elephant, (2) bison, (3) giraffe IL-4 with another associated product, (4) rhinoceros, (M) is the DNA ladder marker, (5) the giraffe IL-4 associated product re-amplification using the inner primer pair and (6) resembles Hartmann's mountain zebra.

IL-4 ORFs lengths were 414 bp for all of the equids, 420 bp for Indian rhinoceros, 408 bp for all of the bovids, 405 for Asian elephant and 402 for the Nubian giraffe, with deduced amino acid sequences of 137 aa for the equids, 139 aa for Indian rhinoceros, 135 aa for the bovids, 134 aa for Asian elephant and 133 aa for Nubian giraffe (table 2).

Table (2) IL-4 cDNA and amino acids lengths of different species:

| Species | ORF | Amino acids |
|---|--------|-------------|
| Human | 462 bp | 153 aa |
| Equids (horse, Somali wild ass and Hartmann's mountain zebra) | 414 bp | 137 aa |
| Indian rhinoceros | 420 bp | 139 aa |
| Bovids (European bison and African buffalo) | 408 bp | 135 aa |
| Asian elephant | 405 bp | 134 aa |
| Nubian giraffe | 402 bp | 133 aa |
| Giraffe IL-4 splice variant | 354 bp | 117 aa |
| Mouse | 423bp | 140 aa |

Legend to table (2)

IL-4 ORFs lengths varied among different families and subsequently provided variable deduced amino acid lengths.

Alignment methods based on sequence similarity are nowadays well developed and have become the commonly used approaches to study species relationship and phylogenomic patterns from genomic sequences. Thereby, homology analysis of nucleotides and deduced amino acid sequences of IL-4 were studied. Although IL-4 ORFs lengths were not equal among species, the interspecies relationships were evident and conservation among animals in the same order (Fig. 6, 7 and 8) was proven through the IL-4 amino acid pairwise analysis (table 3). Phylogenetic profile of IL-4 sequences provided a substantial degree of homology among equids and extended to the species within the order *Perissodactyla*, namely the Indian rhinoceros. A significantly high homology was also detected among artiodactyls (*Bovidae* and Nubian giraffe). Besides, an extreme homology reflected the close relationship among bovids. While the homology between humans and any of the animal species analysed was 62-64%, mice displayed only 52-56% homology (table 3). High homology was also found between perissodactyls and artiodactyls.

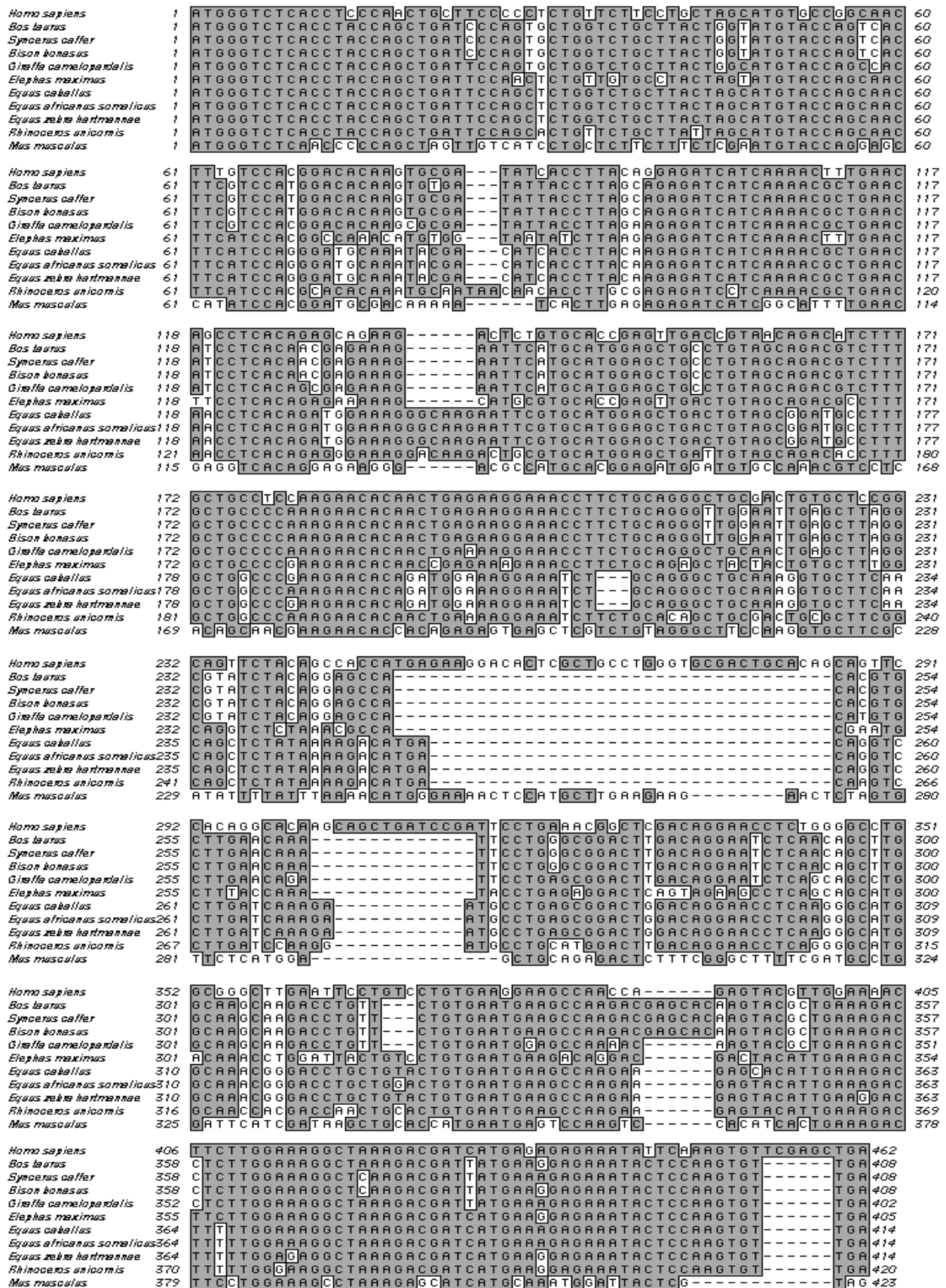


Fig. 6 Comparison of IL-4 ORF cDNA..

The IL-4 cDNAs of cloned mammalian species were compared to that of the reported sequences of human (GenBank: M13982), mouse (M25892) and bovine (M77120). Nucleic acid identities are grey coloured, while variations are white in colour. The differences, in particular between member of different families or orders are clearly visible.

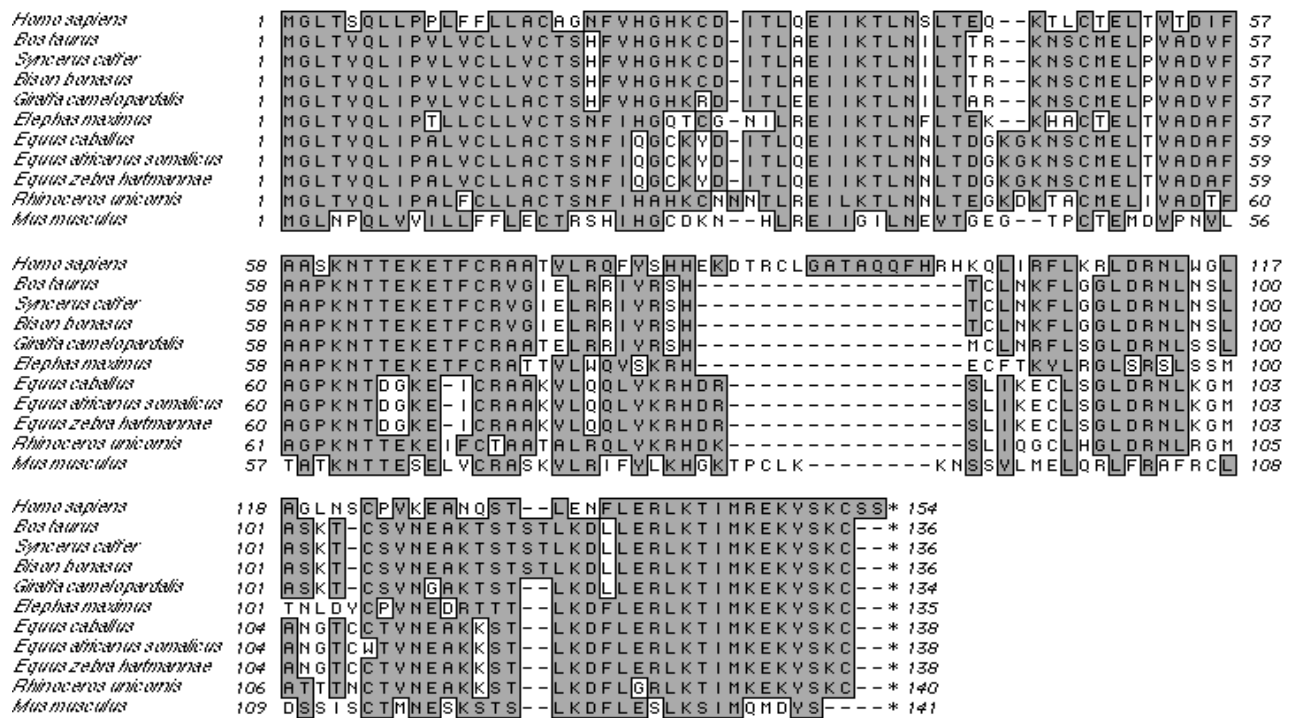


Fig. 7 Alignment of IL-4 protein sequences.

The IL-4 predicted amino acids of cloned mammalian species were aligned with further reported sequences of human, bovine and mouse. Obvious homology is observed among equids and their close relation with rhinoceros is evident. Likewise, close homology is evident among bovinds. Overall, close relationship occurs among artiodactyls' proteins.

Phylogenetic analysis provided a visual account how closely related species are one to one another. Despite variability's among IL-4 ORFs sizes, phylogenetic analysis delineated the same interspecies relationships and clusters as for IFN γ (Fig. 8).

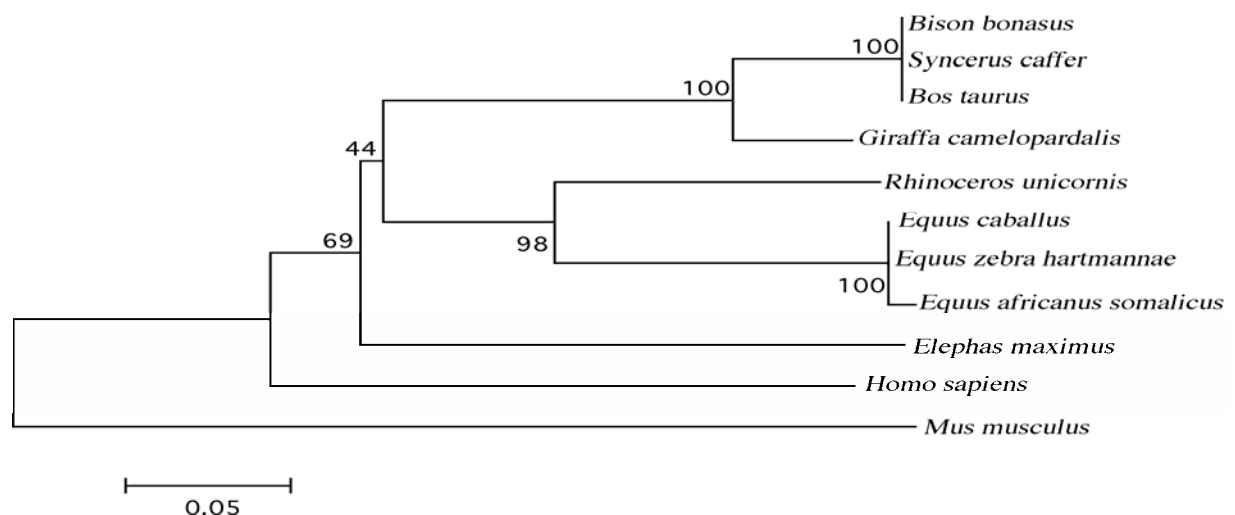


Fig. 8 Phylogenetic relationships between animal species based on IL-4 amino acid sequences.

The deduced amino acid sequences alignment was carried out using MEGA3 software package and Neighbour joining tree with Bootstrap (1000 replicates) analysis and gaps distributed proportionally to analyse phylogenetic relation of IL-4 protein sequences. Horizontal branches were drawn to scale. Bar, 0.05 aa substitutions per site. Mouse IL-4 was used as an out-group. The artiodactyls grouped together with two major branches the first containing all members of family Bovidae and the second only the Nubian giraffe. Alike, perissodactyls clustered together and were divided into Equidae and the Indian rhinoceros as a sole analysed member of the family Rhinocerotidae. The Asian elephant remained unrelated to these groups.

Table (3) IL-4 protein pairwise analysis:

| Human | Bovine | African buffalo | European bison | Nubian giraffe | Asian elephant | Horse | Somali wild ass | Hartmann's zebra | Indian rhinoceros | Mouse | Species |
|-----------|-----------|-----------------|----------------|----------------|----------------|-----------|-----------------|------------------|-------------------|-----------|----------------------------------|
| 100 (100) | 62 (55) | 62 (55) | 62 (55) | 64 (57) | 63 (52) | 64 (53) | 64 (53) | 64 (53) | 64 (55) | 52 (37) | <i>Homo sapiens</i> |
| | 100 (100) | 100 (100) | 100 (100) | 90 (89) | 75 (64) | 73 (66) | 72 (65) | 73 (66) | 74 (64) | 53 (39) | <i>Bos taurus</i> |
| | | 100 (100) | 100 (100) | 90 (89) | 75 (64) | 73 (66) | 72 (65) | 73 (66) | 74 (64) | 53 (39) | <i>Syncerus caffer</i> |
| | | | 100 (100) | 90 (89) | 75 (64) | 73 (66) | 72 (65) | 73 (66) | 74 (64) | 53 (39) | <i>Bison bonasus</i> |
| | | | | 100 (100) | 77 (64) | 75 (68) | 75 (68) | 75 (68) | 74 (65) | 54 (39) | <i>Giraffa camelopardalis</i> |
| | | | | | 100 (100) | 71 (63) | 71 (63) | 71 (63) | 72 (64) | 53 (40) | <i>Elephas maximus</i> |
| | | | | | | 100 (100) | 99 (99) | 100 (100) | 84 (76) | 56 (39) | <i>Equus caballus</i> |
| | | | | | | | 100 (100) | 99 (99) | 83 (75) | 55 (38) | <i>Equus africanus somalicus</i> |
| | | | | | | | | 100 (100) | 84 (76) | 56 (39) | <i>Equus zebra hartmannae</i> |
| | | | | | | | | | 100 (100) | 54 (40) | <i>Rhinoceros unicornis</i> |
| | | | | | | | | | | 100 (100) | <i>Mus musculus</i> |

Legend to table (3)

High homology (identity and similarity) among bovids (blue) and equids (green) was evident. Close relationship was found between equids and Indian rhinoceros alike. While, mice share only little degree of homology with any of the analysed species, human protein was at least 62% homologous. Percentages of homology were calculated by pairwise amino acid sequence alignment using MacVector software package. Numbers are percentage homology with percentage identity provided in brackets.

4.1.2.1 Giraffe IL-4 splice variant

In case of giraffe, a second band significantly smaller in size was most evident in RT-PCR (Fig. 9-A). This band was cut, cloned and sequenced. Sequencing revealed that this smaller sized band described an alternative splice variant (IL-4 δ 2), where the second of four exons was omitted (Fig. 10 and 11). Such alternative splicing of pre-mRNAs is a powerful and versatile regulatory mechanism that can exert control of gene expression and functional diversification of IL-4 proteins.

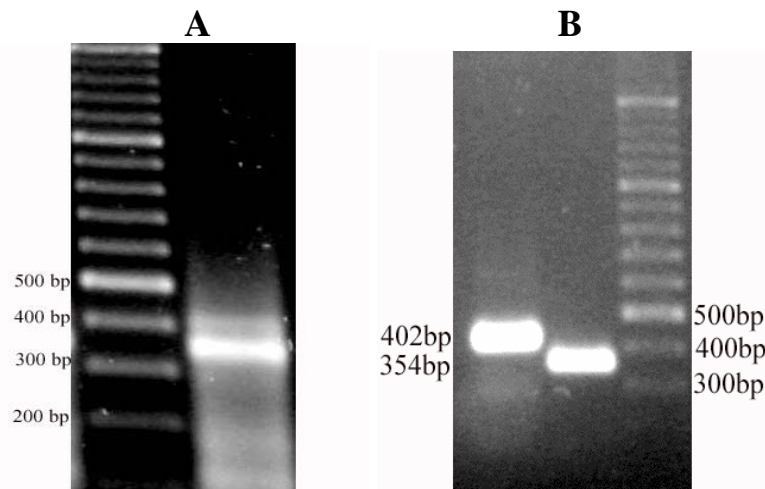


Fig. 9 Giraffe IL-4 splice variant.

Fig. 9-A Giraffe IL-4 nested RT-PCR products agarose gel electrophoresis. Lane 1 is the 100 bp DNA ladder marker and lane 2 contains two bands, where giraffe complete IL-4 ORF appears as a faint band above an obviously and well-displayed strong lower band of the IL-4 splice variant.

Fig. 9-B Clean-up of giraffe IL-4 and giraffe IL-4 splice variant. Lane 1 is giraffe IL-4 cleaned-up, lane 2 Giraffe IL-4 splice variant and lane 3 is the 100 bp DNA ladder marker.

While giraffe complete IL-4 ORF sequence consisted of 402 bp, its splice variant missing the entire second exon consisted only of 354 bp (Fig. 10), with the deduced amino acid sequences of 133 and 117, respectively (Fig. 11).

| | | | |
|---------------------|-----|---|-----|
| Giraffe IL-4 | 1 | ATGGGTCTCACCTACCAGCTGATTCAGTGCTGGTCTGCTTACTGGCATGTACCAGCCAC | 60 |
| Giraffe IL-4 splice | 1 | ATGGGTCTCACCTACCAGCTGATTCAGTGCTGGTCTGCTTACTGGCATGTACCAGCCAC | 60 |
| Giraffe IL-4 | 61 | TTCGTCCACGGACACAGCGCGATATTACCTTAGAAGAGATCATCAAACGCTGAACATC | 120 |
| Giraffe IL-4 splice | 61 | TTCGTCCACGGACACAGCGCGATATTACCTTAGAAGAGATCATCAAACGCTGAACATC | 120 |
| Giraffe IL-4 | 121 | CTCACAGCGAGAAAGAAATTCATGCATGGAGCTGCCTGTAGCAGACGTCCTTGCTGCCCC | 180 |
| Giraffe IL-4 splice | 121 | CTCACAGCGAGAAAGAA----- | 137 |
| Giraffe IL-4 | 181 | AAGAACACAACCTGAAAAGGAACCTTCTGCAGGGCTGCAACTGAGCTTAGGCGTATCTAC | 240 |
| Giraffe IL-4 splice | 138 | -----CACAACTGAAAAGGAACCTTCTGCAGGGCTGCAACTGAGCTTAGGCGTATCTAC | 192 |
| Giraffe IL-4 | 241 | AGGAGCCACATGTGCTTGAACAGATTCCCTGAGCGGACTTGACAGGAATCTCAGCAGCCTG | 300 |
| Giraffe IL-4 splice | 193 | AGGAGCCACATGTGCTTGAACAGATTCCCTGAGCGGACTTGACAGGAATCTCAGCAGCCTG | 252 |
| Giraffe IL-4 | 301 | GCAAGCAAGACCTGTTCTGTGAATGGAGCCAAACAAAGTACGCTGAAAGACCTCTTGGAA | 360 |
| Giraffe IL-4 splice | 253 | GCAAGCAAGACCTGTTCTGTGAATGGAGCCAAACAAAGTACGCTGAAAGACCTCTTGGAA | 312 |
| Giraffe IL-4 | 361 | AGGCTAAGACGATTATGAAGAGAAATACTCCAAGTGTGGA | 402 |
| Giraffe IL-4 splice | 313 | AGGCTAAGACGATTATGAAGAGAAATACTCCAAGTGTGGA | 354 |

Fig. 10 Alignment of giraffe IL-4 and IL-4 δ 2 ORF nucleic acids sequences.

The upper row represented the complete ORF of about 402 bp and the lower represented its splice variant, which consisted only of 354 bp.

| | | | |
|----------------------------|----|--|-----|
| Giraffe IL-4 | 1 | MGLTYQLIPVLVCLLACTSHFVHGHRDITLEEIIKTLNILTARKN | 46 |
| Giraffe IL-4 splice | 1 | MGLTYQLIPVLVCLLACTSHFVHGHRDITLEEIIKTLNILTARKN | 46 |
| Giraffe IL-4 | 47 | SCMELPVADVFAAPKNTTEKETFCRAATELRRIYRSHMCLNRFLSG | 92 |
| Giraffe IL-4 splice | 47 | -----TTEKETFCRAATELRRIYRSHMCLNRFLSG | 76 |
| Giraffe IL-4 | 93 | LDRNLSSLASKTCSVNGAKTSTLKDLLERLKTIMKEKYSKC* | 134 |
| Giraffe IL-4 splice | 77 | LDRNLSSLASKTCSVNGAKTSTLKDLLERLKTIMKEKYSKC* | 118 |

Fig. 11 Alignment of complete giraffe IL-4 and IL-482 amino acid sequences.

While giraffe complete IL-4 consisted of 133 amino acids, the splice variant was only 117 amino acids long.

4.2 Cytokine protein expression

In order to obtain bioactive proteins of both IFN γ and IL-4 from horses, expression cloning in insect cells was attempted. IFN γ induces the expression and up-regulation of MHC genes. In particular, it up-regulates the expression of MHC II on monocytes (Steinbach et al., 2002). IL-4 on the other hand, has been found to affect the phenotype and a variety of functions of monocytes and macrophages, thus inducing down-regulation of CD14 as well as alteration in monocyte morphology (Lauener et al., 1990; Peters et al., 1996).

Accordingly, in order to detect the bioactivity of recombinant eqIFN γ , isolated horse monocytes were treated with the insect cell-expressed eqIFN γ . Thereafter monocytes were analysed using a mAb against equine anti-MHC II, followed by PE-conjugated anti-mouse secondary Ab and analysed by flow cytometry. Within 24 hours an effect of IFN γ was most obvious (Fig. 12).

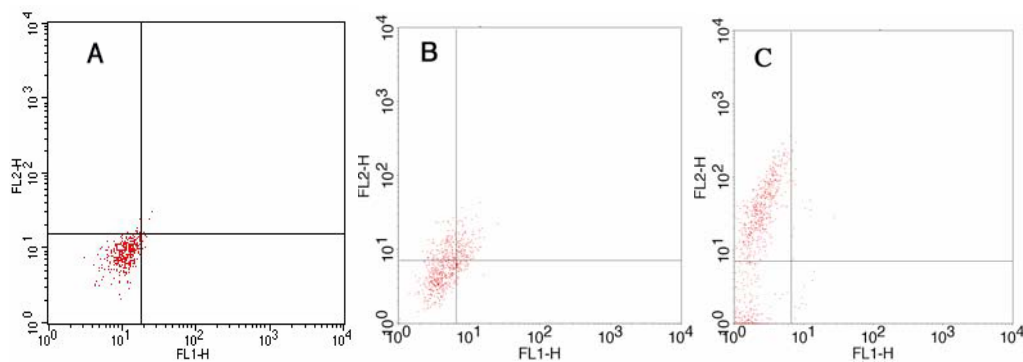


Fig. 12 Effect of eqIFN γ MHC II expression on horse monocytes.

Fig. 12-A was the isotype negative control.

Fig. 12-B were non-treated horse monocytes (negative control) at day one.

Fig. 12-C represented the eqIFN γ -treated monocytes after the same time.

In order to detect the bioactivity of expressed equine IL-4, isolated horse monocytes were treated with supernatants of recombinant eqIL-4 insect cells transfectants and monitored for morphological alterations (Fig. 13) and CD14 regulation (data not shown).

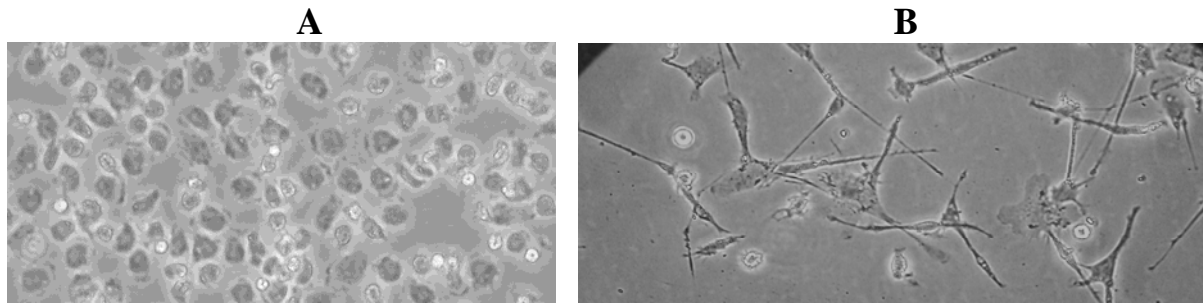


Fig. 13 Effect of expressed eqIL-4 on horse monocytes.

Fig. 13-A Non-treated monocytes were used as negative control.

Fig. 13-B EqIL-4 induced monocyte transformation to cells with long dendrites within 48 hours.

Flow cytometric analysis of cultured horse monocytes demonstrated that cells incubated in the presence of IL-4, revealed a reduced expression of the CD14 antigen. Unfortunately, this attempt to quantify the effect of eqIL-4 on CD14 expression did not provide a constant result sufficient to allow quantification of IL-4 (data not shown). Besides, trichloroacetic acid/deoxycholate (TCA/DOC) was used to concentrate expressed equine IL-4 proteins in order to overcome the low-concentration of protein in insect cell supernatants. Thereafter, this concentrated eqIL-4 proteins were separated by sodium dodecyl sulphate poly acrylamide gel electrophoresis (SDS-PAGE) before being visualized by silver staining. The concentrated eqIL-4 proteins included a band of the predicted molecular mass of approximately 17.8 kDa (Fig. 14).

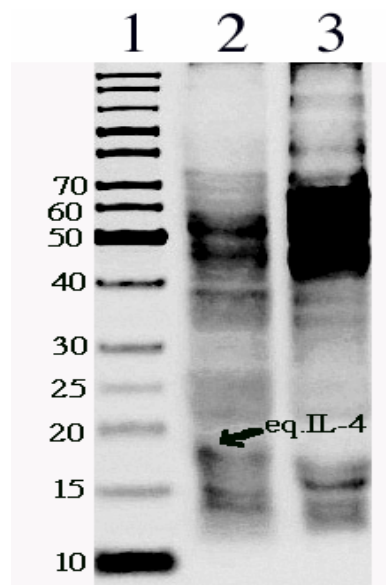


Fig. 14 The recombinant eqIL-4 protein.

SDS-Polyacrylamide gel electrophoresis (SDS-PAGE) of insect expressed and subsequently concentrated horse IL-4. Lane 1 is a PageRuler. Lane 2 is the expressed horse IL-4 protein containing a band of approximately 17.8 kDa. Lane 3 is the High Five negative control supernatant.

4.3 Quantification of IFN γ and IL-4 mRNA expression

Introduction of a fluorescence-kinetic based PCR enabled direct quantification of the PCR product in 'real-time'. This technique measures the PCR product accumulation during the exponential phase of the reaction, and thereby avoids post-PCR manipulations. Since its introduction, this method has been more and more widely used. The aim of this part of the thesis was to establish a real-time PCR that can determine IFN γ and IL-4 mRNA expression levels in parallel. This test could be used to generate immune profiles against both intracellular and extracellular infections. As a model, I used equine IFN γ and IL-4 since sufficient material was available from horses.

4.3.1 Establishing real-time RT-PCR assays for equine IFN γ and IL-4

In order to establish real-time PCR assays measuring IFN γ and IL-4 mRNA expression, sequence-specific primers and probes were designed for the horse. In SYBR-green assays, each of the primer pairs was first tested for its fitness (efficiency) with plasmids containing the cDNA as a positive control (data not shown). Thereafter, the reactions were optimized and tested over a range of plasmid serial dilutions (from 10^{-5} to 10^{-11}) for IFN γ and (from 10^{-6} to 10^{-11}) for IL-4 (Fig. 15 and 16).

In real-time PCR analysis, quantification is based on the C_t (threshold cycle), defined as the first amplification cycle in which the fluorescence indicating PCR products becomes detectable in the exponential phase of PCR. The C_t is determined at the early exponential phase of the reaction and is more reliable than end-point measurements of accumulated PCR products used by traditional PCR methods. The C_t is inversely proportional to the copy number of the target template; the higher the template concentration is, the lower the threshold cycle measured. All experiments were performed in triplicates and each experiment was at least performed three times with analogous results, of which one experiment is displayed.

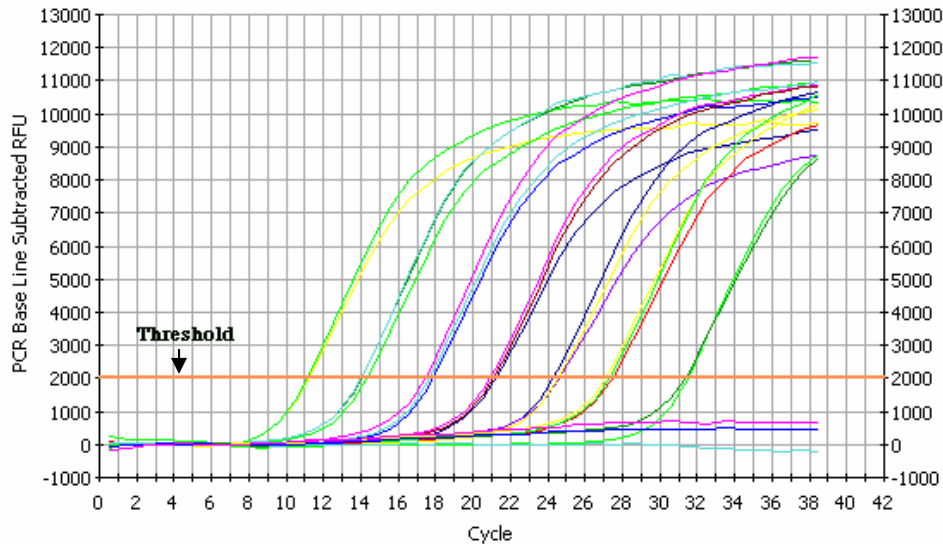


Fig. 15 Real-time PCR of horse IFN γ plasmid.

Serial dilutions of horse IFN γ plasmid over 7 magnitudes between 10^{-5} and 10^{-11} were quantified using SYBR-green real-time PCR. For quality control, all reactions were set up in triplicate. Here, triplicates were analysed individually, each plot represents an individual data set. Cycle numbers are shown along the X-axis and arbitrary fluorescence units are shown on the Y-axis. Quantitative real-time PCR measures the cycle number at which the increase in fluorescence is significant. The point at which the fluorescence crosses the so-called threshold is called the C_t . More diluted samples cross the threshold at higher C_t values. Negative (water) controls do not cross the threshold at all.

The IFN γ stock plasmid concentration was estimated as 9.0×10^9 molecules/ $1\mu\text{l}$ (3.2.6.2). Alike, IL-4 stock plasmid concentration was determined as 6.6×10^9 molecules/ $1\mu\text{l}$. Since the detection range of IFN γ and IL-4 plasmid dilution reached 10^{-11} (Fig. 15 and 16), both real-time assays detected plasmid copy numbers around one molecule for IFN γ and IL-4 cDNA, each.

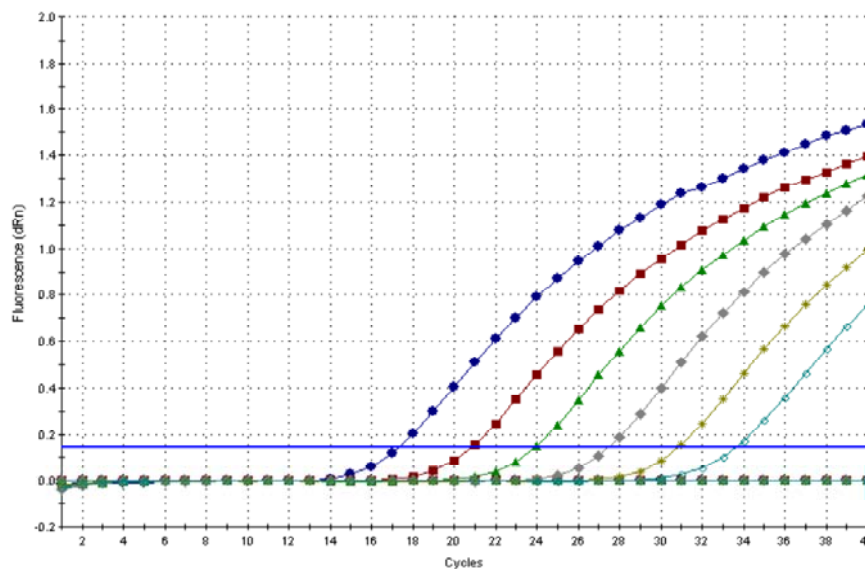


Fig. 16 Real-time PCR of horse IL-4 plasmid.

Serial dilutions of horse IL-4 plasmid over 6 orders of magnitudes between 10^{-6} and 10^{-11} were quantified using SYBR-green real-time PCR. All reactions were set up in triplicate, thereafter first analyzed individually and then collectively as displayed. Cycle number is shown along the X-axis and baseline-corrected normalized fluorescence (dRn) on the Y-axis. Dark green dotted line is the water control.

SYBR-green is a double-stranded DNA (dsDNA) binding dye, which is incorporated in the amplicon during the real time PCR. Since SYBR-green does not distinguish between the target-DNA and any other (unspecific) DNA, one way of quality control is to check the melting temperature as SYBR-green dissociation curve. All products generated during PCR amplification reaction are first melted at 95°C, then annealed at 55°C and subjected to gradual increases (0.5°C) in temperature. After each incremental temperature change, fluorescence data are collected until the reaction reaches 95°C. The result is a plot of fluorescence units *versus* temperature.

SYBR-green dissociation curves were run for both of eqIFN γ and eqIL-4 designed primer sets using cDNA from activated horse PBMC as test samples. The melting curve should result in a single peak, which distinguishes a specific reaction from unspecific background signals. Accordingly, obtained dissociation curves revealed high specificity of each of the used primer sets (Fig. 17). Additionally, an agarose gel check was performed where no additional bands were detected (data not shown).

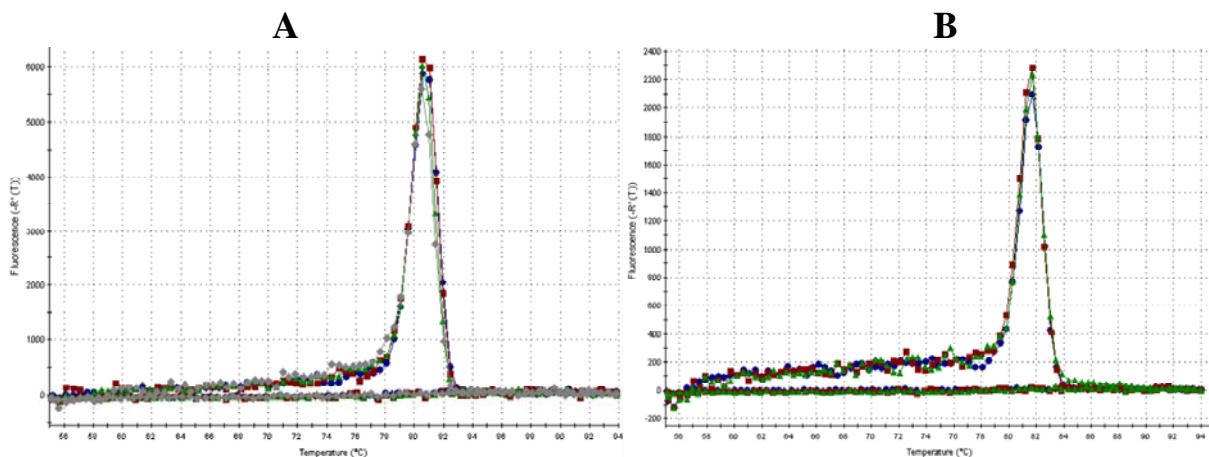


Fig. 17 IFN γ (A) and IL-4 (B) SYBR-green dissociation curves.

Displayed as $\Delta\text{RFU}/\Delta\text{T}$ derived curve where ΔRFU is the difference in relative fluorescent units (RFU) and ΔT is the difference in (dissociation) temperature.

The single melt peak at around 80°C for IFN γ (Fig. 17-A) and 81.0°C for IL-4 (Fig. 17-B) indicated a single PCR product being amplified during real-time PCR from horse cDNA.

All these tests using SYBR-green were performed for all Metabion and TIB MOLBIOL primer pairs listed in material and methods (3.2.6) and provided identical results with regard to specificity and analogous results for the sensitivity.

TaqMan real-time PCR

TaqMan probes are linear oligonucleotides of 15-30 bp, which are designed to allow close proximity of a fluorophore (e.g. 6-carboxy-fluorescein) and its quencher (e.g. 6-carboxy-tetramethyl-rhodamine) in the intact, unstructured probe. As long as the probe is intact, no

fluorescence is observed from the fluorophore. During the annealing–extension step of the real-time PCR, the DNA polymerase displaces the TaqMan probe by 3 or 4 nucleotides, and the 5′ nuclease activity of the DNA polymerase releases the fluorophore from the quencher. Fluorescence can be detected during each PCR cycle and it accumulates during the course of PCR. Optimization of the PCR reaction is required for the primers as well as probe set. Here, standard curves and correlation coefficients were analysed to check experiment efficiency and quality of the real-time PCR.

The standard curve is a plot of 10 fold template dilutions plotted *versus* C_t values. The result should be a linear graph. Standard curves are generally accepted when the slopes were between -3.7 and -3.3 (corresponding to PCR efficiencies of between 85 and 100%) and correlation coefficients (r^2) were >0.990 . The (r^2) value is a calculated assessment of the fitting of the standard curve to the data points plotted. The closer r^2 is to 1, the better the data points fit the line.

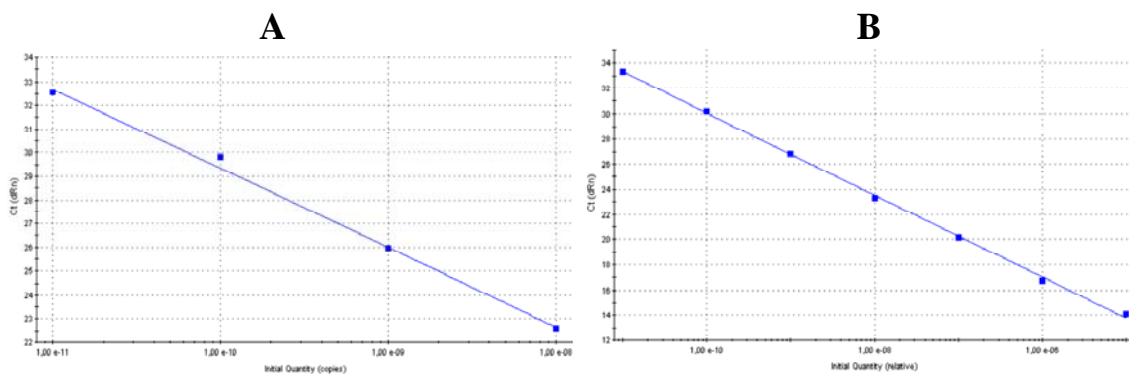


Fig. 18 Standard curves for horse IFN γ (A) and IL-4 (B).

Fig. 18-A Serial dilutions of horse IFN γ plasmid over four orders of magnitude between 10^{-8} and 10^{-11} were used as template. Each point represents the mean of three replicates of one sample. Here, $r^2 = 0.998$ and the slope = -3.3, corresponding to a PCR efficiency of 99.0%.

Fig. 18-B Seven orders of magnitude serial dilutions of horse IL-4 plasmid between 10^{-5} and 10^{-11} were used as template. Each point represents the mean of three replicates of one sample. Here $r^2 = 0.999$ and the slope = -3.3, corresponding to a PCR efficiency of 102.4%

The standard curves for IFN γ (Fig. 18-A) and IL-4 (Fig. 18-B) were clearly acceptable.

Endogenous normalizer is one of the most important experimental controls that must be included in gene-expression assays. It is used to normalize the signal value of each sample so that differences between samples are the result of a real biological difference and not of an inconsistent amount. Normalizers are also known as the internal control. Housekeeping genes are the typical choice due to their mostly consistent expression levels in all cell types. Glyceraldehyde 3-phosphate dehydrogenase (GAPDH), β -actin, cyclophilin and 18S rRNA are the commonly used. Both GAPDH and β -actin have been shown to vary with numerous conditions (Suzuki et al., 2000) and are not the best choice. Cyclophilin expression is equal

among most tissues, with the exception of heart and muscle. 18S rRNA was chosen here because of its relatively invariant level among tissues and treatment conditions.

To test the expression level of 18S rRNA, equal amounts of horse PBMC were activated with PMA (0.1 $\mu\text{g/ml}$ cell suspension) for different durations (24 and 48 hours) and unstimulated cells were taken as negative control. Whole cellular RNA was extracted, reverse transcribed using random hexamer primers and 18S rRNA expression levels were tested using absolute quantitative real-time PCR. Amplification plots of 18S rRNA were very close to each other over the first 24 hours. The little expression difference in the second 24 hours was likely due to the morphologically observed proliferation of cells, thus indicating 18S expression stability per cell (Fig. 19-A). In addition, horse PBMC were tested for their expression of IFN γ and IL-4 as genes of interest compared to 18S rRNA. Due to its very high expression, 18S was detected at much lower C_t than IFN γ and IL-4. The chosen 18S detection kit has therefore a primer limitation, which allows its use in multiplex assays and results in comparatively inefficient end point amplification (Fig. 19-B).

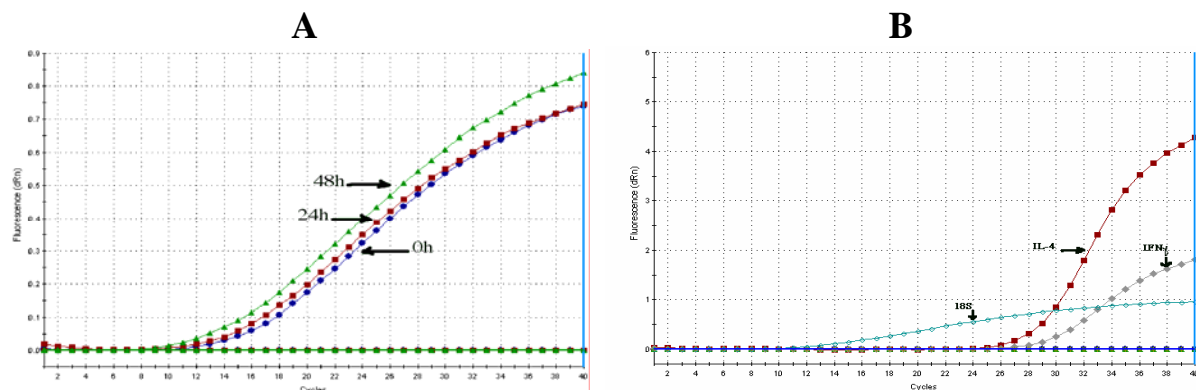


Fig. 19 Expression levels of 18S rRNA.

Fig. 19-A Stability of 18S rRNA expression. PMA activated cells were tested at different incubation times. Plots in green triangles indicate 48 hours, reddish-brown quadrants 24 hours and blue dots zero hour (threshold not shown).

Fig. 19-B Comparative expression levels of IFN γ , IL-4 and 18S rRNA in nonactivated horse PBMC using TaqMan assays. The amplification plot of IFN γ is displayed grey, IL-4 red and 18S light blue, using TaqMan protocol in absolute quantification real-time PCR (threshold not shown).

In order to further optimize real-time PCR conditions, the same eqIL-4 primers and probe were used with TaqMan PCR reaction mix of different sources (Qiagen, Stratagene and Invitrogen) in absolute quantification real-time PCR according to each manufacture's instructions.

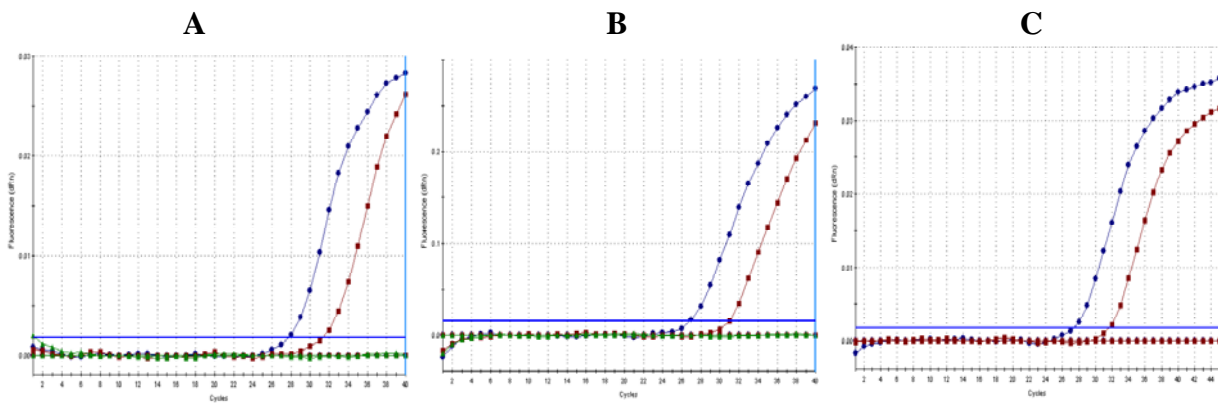


Fig. 20 Comparison of the TaqMan mix of different sources.

A plasmid containing eqIL-4 cDNA was used at a dilution of 10^{-8} and 10^{-9} .

Fig. 20-A: Threshold cycles were 28 and 31 using Qiagen TaqMan mix.

Fig. 20-B: Threshold cycles were 27 and 31 using Stratagene brilliant TaqMan master mix.

Fig. 20-C: Threshold cycles were 28 and 32 using Invitrogen TaqMan mix.

Each plot represents the mean of three replicate measurements of one sample.

The data obtained revealed no significant differences. Further experiments were performed using the Stratagene brilliant TaqMan master mix.

In order to compare the sensitivity of SYBR-green and TaqMan assays, a serial dilution of equine IL-4 cDNA plasmid was subtracted to both tests in parallel. When data were displayed in the same graph it became evident that the SYBR-green assay was significantly more sensitive than the TaqMan assay, as demonstrated by the lower C_t values (Fig. 21). However, the detection limits for both IL-4 and IFN γ cDNA *via* TaqMan assays were still below 10 copies each (data for IFN γ not shown).

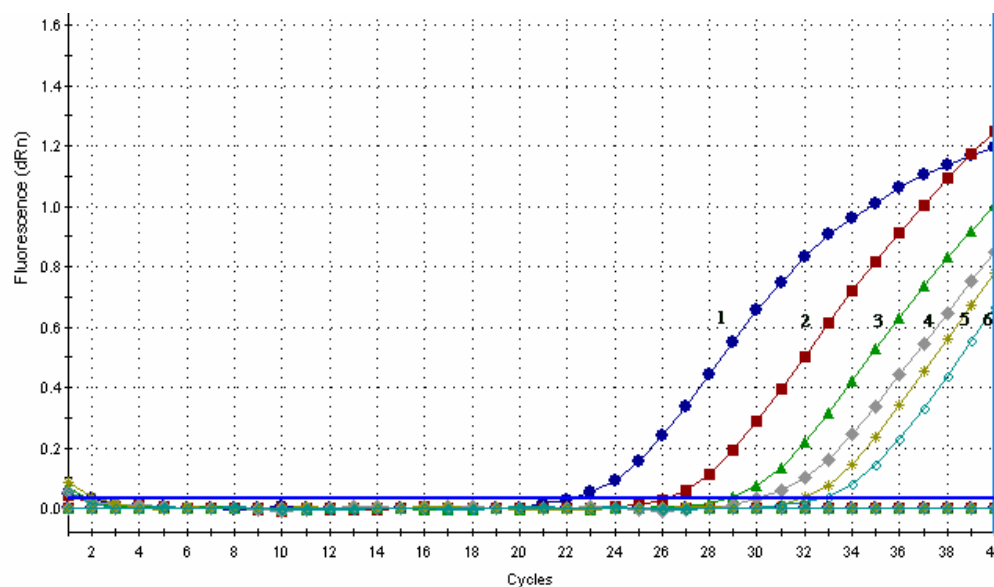


Fig. 21 Comparison of TaqMan *versus* SYBR-green assays in absolute quantitative real time PCR.

Three orders of magnitude serial dilutions of horse IL-4 plasmid between 10^{-9} and 10^{-11} were used as template in absolute quantification real-time PCR. SYBR-green resulted in amplification plots with significantly lower C_t values (1, 2 and 3) compared to TaqMan probe amplification plots (4, 5 and 6).

Despite the data obtained from the comparison between TaqMan and SYBR-green, it was decided to use TaqMan probe in the objected diagnostic assay to allow further application in multiplex real-time PCR. Besides, the experiment displayed in Fig. 19-B had shown that both IFN γ and IL-4 TaqMan assays allowed the detection of mRNA from unstimulated cells, which was the baseline of the assay to be established.

Application of real-time PCR in T-cell activation assays:

Ligation of T-cell receptors (TCR) by antigen-MHC complexes on antigen presenting cells (APCs) triggers T cell activation. A second signal, mediated by the interaction with CD28 or other co-stimulatory molecules, is *in vivo* required for the full activation. T-cell activation induces two major signal transduction pathways, the protein kinase C (PKC)-mitogen-activated protein kinase (MAPK) pathway and the calcium-dependent calcineurin-mediated pathway. A frequently used artificial stimulus for T-cells is PMA + ionomycin, which act by increasing cytoplasmic Ca⁺² concentration and activating protein kinase C. Alternatively, antibodies directed against CD3 (as part of the TCR complex) might be used for T-cell activation *in vitro*. Antibodies to CD28 can augment the proliferation of T-cells stimulated with suboptimal doses of mitogens or CD3.

PMA and Ca-ionophore or anti-CD3, are at higher concentrations each independently able to induce T-cell activation on their own. To determine the optimal and suboptimal activation conditions, time kinetic and concentration experiments were performed with horse lymphocytes using the real-time PCR for IFN γ as readout.

The optimal time of PMA induced T-cell activation was analysed in two steps. The first step was carried out in long intervals (6 hours) (Fig. 22-A) followed by a second step of shorter intervals of 1-2 hours (Fig. 22-B). Expression of 18S rRNA was determined to analyse that mRNA levels were comparable (representing a comparable amount of cells in the experiments, data not shown).

The first data from time kinetic analysis indicated that IFN γ mRNA expression declined with increased stimulation beyond 8 hours. Since amplification plots of 6-8 hours PMA-stimulated horse PBMC resulted in the lowest C_t value, it was considered the best time for PMA stimulation, which was confirmed by the second experiment (Fig. 22-B).

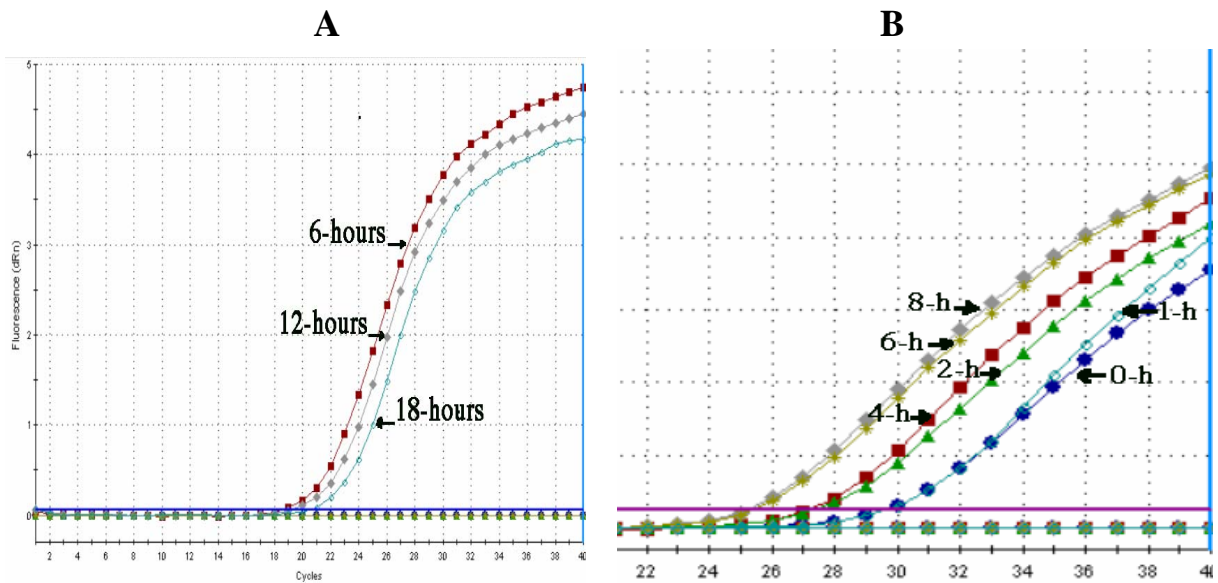


Fig. 22 Time kinetic analysis of IFN γ mRNA expression of horse PBMC stimulated with PMA.

Fig. 22-A In the first experiment, horse PBMC were stimulated with (0.1 $\mu\text{g}/\text{ml}$) PMA for different times (6, 12 and 18 hours). Levels of mRNA IFN γ were determined using absolute quantitative real-time PCR with TaqMan protocol. Amplification plots of IFN γ shown are red quadrants for 6 hours activation, grey quadrants for 12 hours and light blue circles for 18 hours.

Fig. 22-B In the second experiment, horse PBMC were stimulated with the same PMA concentration for different durations (1, 2, 4, 6 and 8 hours) of activation and zero hour PBMC were taken as negative control. Whole RNA was extracted and levels of IFN γ were determined using absolute quantification real-time PCR. Amplification plots of mRNA of IFN γ of the zero-hour are blue dots, 1-hour stimulation are light blue circles, 2-hours are green triangles, 4-hours are red quadrants, 6-hours are khaki asterix and 8-hours is grey quadrants.

Objecting to determine the PMA concentration required for optimal horse PBMC stimulation, an analogous PMA concentration analysis was carried out using variable PMA concentrations for 8 hours. Thereafter, cellular RNA was extracted and levels of IFN γ mRNA were determined in absolute quantitative real-time PCR using TaqMan protocol.

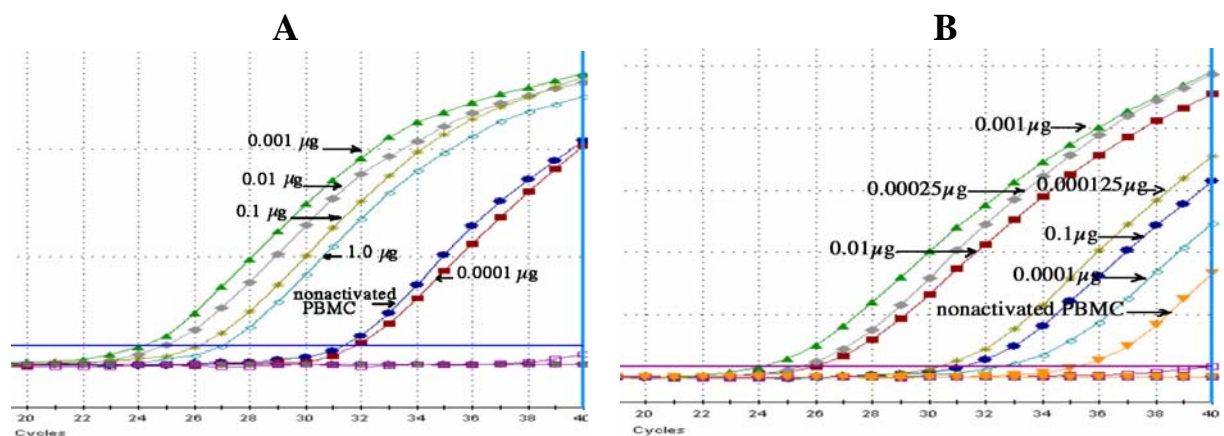


Fig. 23 IFN γ mRNA expression from horse PBMC stimulated with different concentrations of PMA.

Fig. 23-A In the first experiment, horse PBMC activated by PMA 1.00-0.0001 $\mu\text{g}/\text{ml}$ for 8 hours.

Fig. 23-B In the second experiment, horse PBMC were stimulated with slightly modified PMA concentrations from 0.1 to 0.0001 $\mu\text{g}/\text{ml}$ for 8 hours again.

Overall, PMA stimulation experiments revealed that concentrations of 0.001 $\mu\text{g/ml}$ cell suspension for 6-8 hours were sufficient to induce optimal horse PBMC activation (Fig. 23).

For Ca-ionophore activation the analogous approach as for PMA was used (data not shown). Here, 2 hours of activation was considered the optimum time required and 1.00 $\mu\text{g/ml}$ was considered the best concentration for horse PBMC activation.

4.3.2 Relative quantification of horse IFN γ and IL-4 gene expression

Relative gene quantification analyzes the expression level of a target gene *versus* a reference gene and is adequate for investigating changes in gene expression levels.

In this approach, I compared the C_t values of *in vitro* stimulated PBMC for the expression of IFN γ and IL-4 (as genes of interest) with non-activated PBMC as calibrator (or non-treated sample) control. C_t values of both the calibrator and the samples of interest were normalized to 18S RNA, chosen as an appropriate endogenous housekeeping gene. Relative gene expression was calculated *via* series of calculations in the software package using the C_t values. In brief, the first calculation was to subtract the normalizer 18S rRNA C_t values from the genes of interest C_t (target genes) to produce the ΔC_t values. Thereafter, ΔC_t values of the calibrator (neg. control) were subtracted from the target sample to produce the $\Delta\Delta C_t$ value. The $2^{-\Delta\Delta C_t}$ was determined for every sample as the relative expression level.

Where: $\Delta\Delta C_t = \Delta C_t$ (sample) $- \Delta C_t$ (calibrator)

$\Delta C_t = C_t$ (gene of interest) $- C_t$ (normalizer), and $C_t =$ cycle threshold.

Co-stimulation by anti-CD28 is known to facilitate T cell activation by decreasing the strength of interaction and time of commitment, and protecting T cells from death (Boise et al., 1995; Noel et al., 1996). A polyclonal anti-human CD28 was tested to determine if it exhibits an effect on sub-optimally stimulated equine T-cells as described for human cells (Ledbetter et al., 1990).

Horse PBMC were stimulated with suboptimal concentration of PMA Ca-ionophore (i.e. 0.00025 $\mu\text{g/ml}$ PMA and 0.1 $\mu\text{g/ml}$ Ca-ionophore) for 8 hours and treated with polyclonal anti-human CD28 (1 $\mu\text{g/ml}$). Levels of IFN γ and IL-4 were relatively quantified in TaqMan real-time PCR, normalized to 18S rRNA. The results were displayed in a chart where each column represents the mean of three replicate measurements of one sample (Fig. 24).

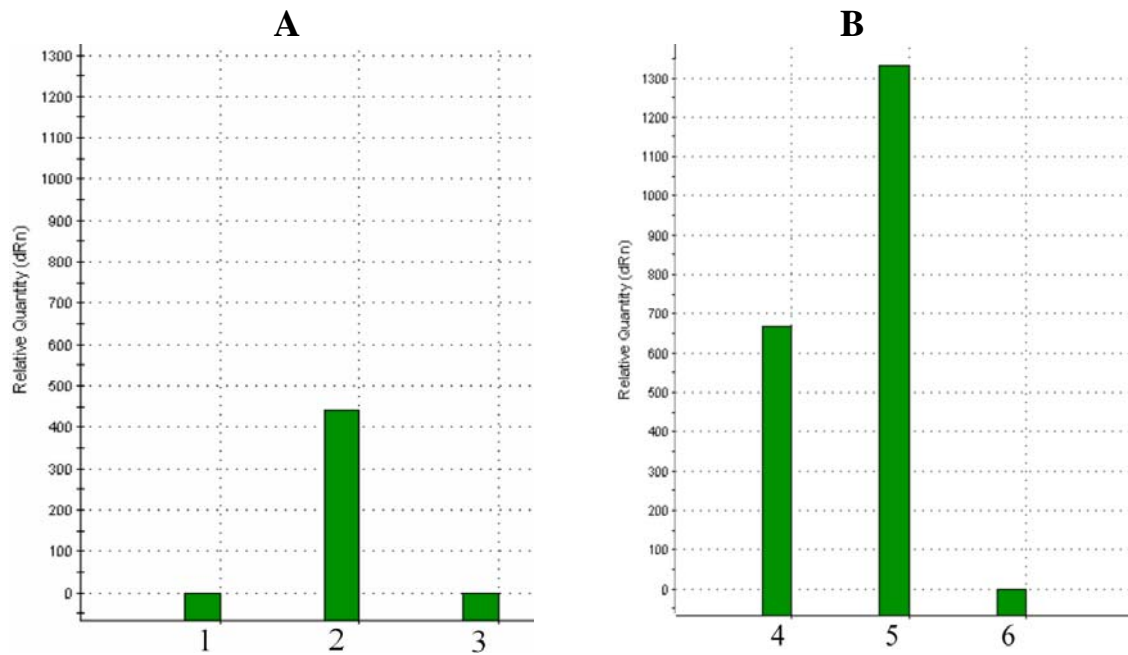


Fig. 24 Effect of polyclonal anti-human CD28 on PMA Ca-ionophore stimulated PBMC regarding IFN γ and IL-4 mRNA expression as measured by real-time PCR.

Fig. 24-A IFN γ mRNA expression levels of the suboptimal PMA/Ca-ionophore stimulation without anti-human CD28 co-stimulation (1), PMA/Ca-ionophore in combination with 1.00 μ g/ml anti-human CD28 as co-stimulator (2), the non-activated PBMC as negative control (3).

Fig. 24-B IL-4 mRNA expression levels of the suboptimal PMA/Ca-ionophore stimulation without anti-human CD28 co-stimulation (4), PMA/Ca-ionophore in combination with 1.00 μ g/ml anti-human CD28 as co-stimulator (5), the non-activated PBMC as negative control (6).

Since an increase in cytokine mRNA expression was induced by the addition of the anti-human CD28, variable concentrations of anti-CD28 were tested to determine the optimal concentration to be used for horse PBMC (Fig. 25).

Overall, results demonstrated an increase of cytokine mRNA expression by the addition of anti-CD28. Thus, the anti-human CD28 exhibited co-stimulatory effects on horse PBMC, suboptimally primed by PMA/Ca-ionophore. An anti-human CD28 concentration of 1 μ g/ml induced best results. Next, this experimental co-stimulation was tested in the slightly more biological setting of anti-CD3 stimulation.

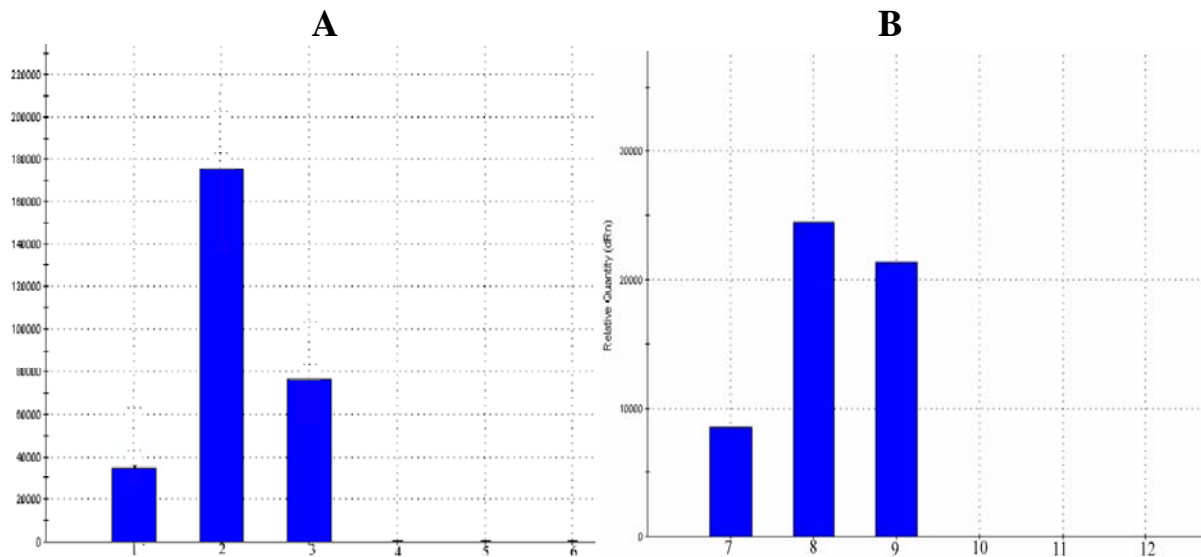


Fig. 25 Variable concentrations of anti-human CD28 with suboptimal PMA/Ca-ionophore activation.

Horse PBMC were stimulated with PMA/Ca-ionophore for 8 hours using varying concentrations of polyclonal anti-human CD28 (0.5, 1.00 and 2.00 $\mu\text{g/ml}$) in order to determine the optimal anti-CD28 concentration to be used. Levels of IFN γ and IL-4 mRNA expression were determined and normalized to 18S RNA in relative quantification real-time PCR using TaqMan protocol.

Fig. 25-A IFN γ mRNA levels after suboptimal PMA Ca-ionophore stimulation with 0.5 $\mu\text{g/ml}$ anti-CD28 (1), 1.00 $\mu\text{g/ml}$ anti-CD28 (2), 2.00 $\mu\text{g/ml}$ anti-CD28 (3). Controls were the non-activated PBMC with anti-CD69 1 $\mu\text{g/ml}$ as negative control (4), non-activated PBMC with anti-CD28 1 $\mu\text{g/ml}$ as a second negative control (5) and non-activated PBMC as calibrator (6).

Fig. 25-B IL-4 mRNA levels after suboptimal PMA Ca-ionophore stimulation with 0.5 $\mu\text{g/ml}$ anti-CD28 (7), 1.00 $\mu\text{g/ml}$ anti-CD28 (8) and 2.00 $\mu\text{g/ml}$ anti-CD28 (9). Controls were the non-activated PBMC with anti-CD69 1 $\mu\text{g/ml}$ as negative control (10), non-activated PBMC with CD28 1 $\mu\text{g/ml}$ as a second negative control (11) and non-activated PBMC as calibrator (12).

4.3.3 Anti-CD3 activation

Some anti-CD3 monoclonal antibodies have potent mitogenic properties, as they are able to cross-link CD3. An anti-equine CD3 mAb has been described earlier (Blanchard-Channell, et al., 1994; Patton et al., 2004).

In order to check whether the anti-equine CD3 monoclonal antibodies possess a self-potent mitogen-like property *via* CD3 cross-linking, anti-CD3 mAb was immobilized to tissue culture plates (Müller, 1998) without co-stimulation and in combination with 1 $\mu\text{g/ml}$ anti-CD28 co-stimulation. mRNA expression levels of IFN γ and IL-4 were determined and normalized to 18S rRNA in relative quantification real-time PCR (Fig. 26).

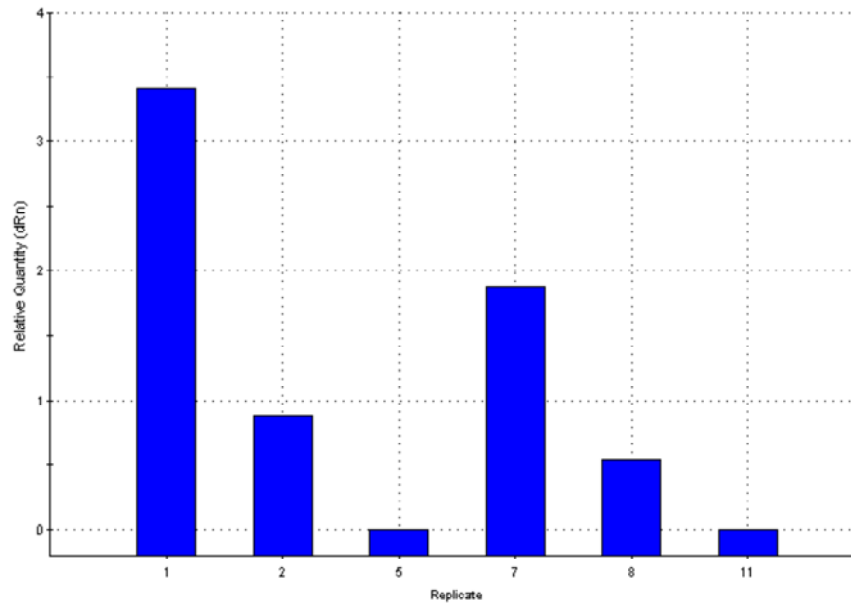


Fig. 26 Anti-equine CD3 priming with anti-human CD28 co-stimulation.

Horse PBMC were stimulated with 1:100 anti-equine CD3 mAb, with and without anti-CD28 (1 μ g/ml) for 48 hours. Total RNA was extracted and levels of IFN γ and IL-4 mRNA were relatively quantified by real-time PCR. Replicate No (1) is IFN γ of 1:100 anti-equine CD3 with 1 μ g/ml CD28, (2) is IFN γ of 1:100 anti-equine CD3 only, (5) is the unstimulated PBMC control, (7) is IL-4 from 1:100 anti-equine CD3 with 1 μ g/ml anti-CD28, (8) is IL-4 of 1:100 anti-equine CD3 only, (11) is IL-4 of the unstimulated PBMC negative control. Normalization was performed against 18S rRNA.

Anti-equine CD3 mAb was used in different dilutions of 1:5, 1:10, 1:20 and 1:100 (data not shown) and incubated for 24-72 hours with co-stimulation of anti-CD28 added at a concentration of 1 μ g/ml, previously found to provide optimal co-stimulatory effect.

Obtained results demonstrated that immobilized anti-equine CD3 mAb (1:100 diluted) incubated for 48 hours induced a PBMC stimulation, which was effectively augmented by the addition of anti-CD28 polyclonal serum (Fig. 27).

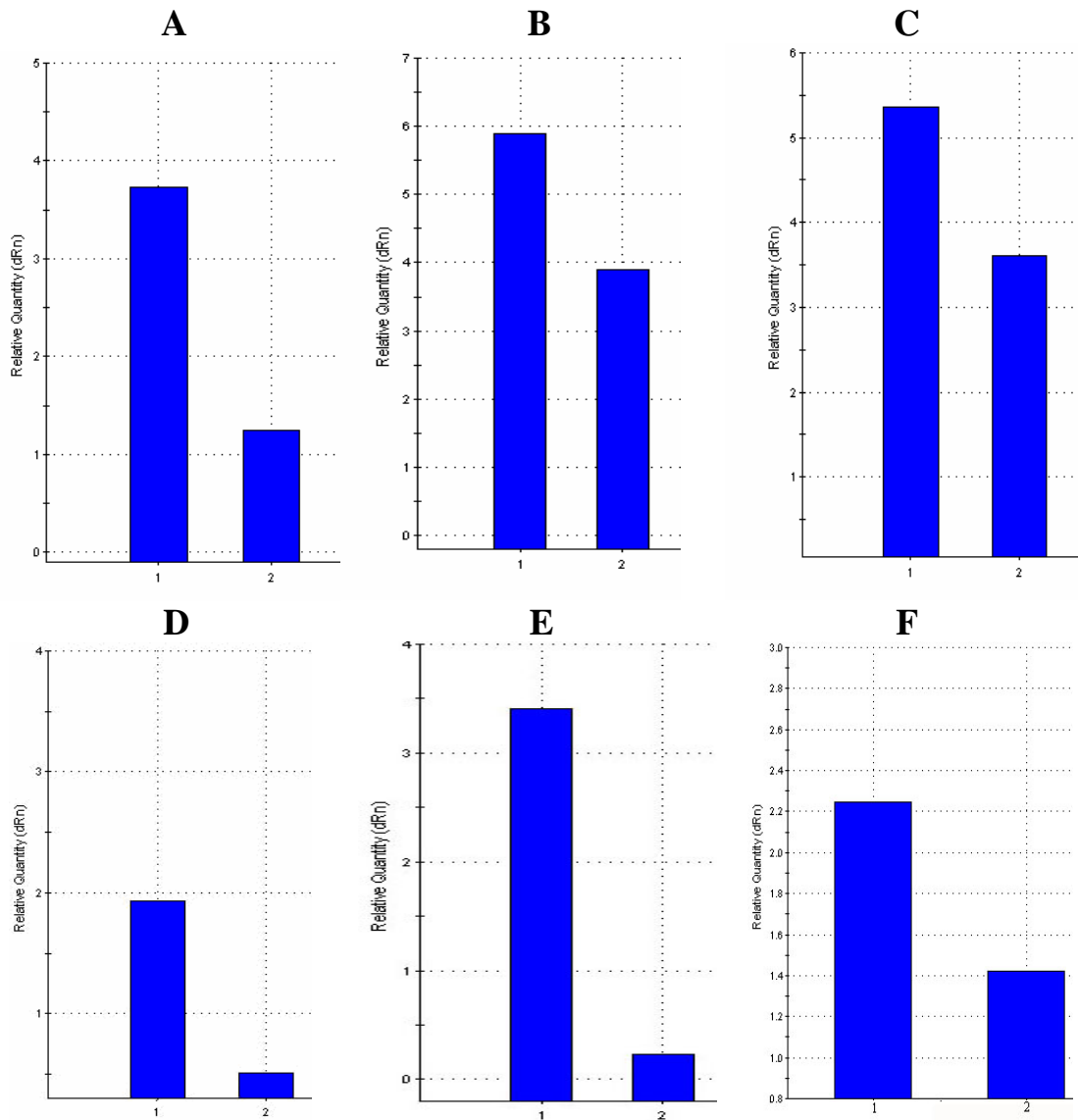


Fig. 27 Time kinetic of anti-equine CD3 with anti-human CD28 co-stimulation.

Horse PBMC were stimulated with immobilized anti-equine CD3 for 24, 48 or 72 hours. Levels of IFN γ and IL-4 mRNA expression were determined in a TaqMan real-time PCR. Immobilized anti-equine CD3 with anti-CD28 co-stimulation (1) and without anti-CD28 (2). While, the upper row represents IFN γ the lower is IL-4 mRNA. Fig. A & D 24 hours, Fig. B & E 48 hours and Fig. C & F 72 hours. Normalization was performed against 18S rRNA.

4.3.4 Antigenic stimulation

Immunological memory is a central feature of the immune response of vertebrates. A recall response to activate circulating memory T-cells does not require more APC than existing in PBMC (Bluestone et al., 1995). Accordingly, a memory response can be measured on freshly isolated PBMC adding antigen and possibly anti-CD28 as co-stimulus (Harding et al., 1992).

4.3.4.1 Equine herpesvirus-1 stimulation

Equine herpesvirus-1 (EHV-1) is a ubiquitous pathogen of horses, well known to be one of the most important infectious pathogens in horses as it can cause abortion in pregnant mares,

early neonatal death in foals, respiratory disease and occasionally neurological disease (Paillot et al., 2006). However, vaccination may reduce the severity of the disease and is commonly used. Thus, inactivated *EHV-1* was used as a specific recall antigen, for which a certain level of immunity was assumed.

Stimulation was performed with *EHV-1*/anti-CD28 for different durations (12, 24 and 48 hours) and inactivated *EHV-1* was used in different concentrations (10, 20, 50, 100, 200 and 400 μ l) corresponding to 10^4 - 4×10^5 PFU/ml with co-stimulation by anti-CD28. mRNA expression levels of IFN γ and IL-4 were determined and normalized to 18S rRNA in relative quantification real-time PCR. The data obtained clearly showed that an antigen-specific recall response could be induced and the readout was best after 12 hours incubation (Fig. 28, data not shown).

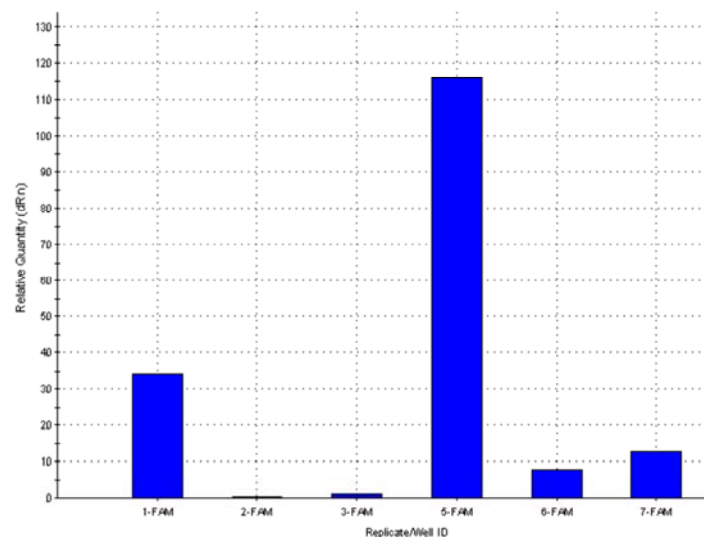


Fig. 28 *EHV-1* stimulation combined with anti-CD28 co-stimulation.

Horse PBMC were stimulated with *EHV-1* (50 μ l/ml) and anti-CD28 (1 μ g/ml) for 12hours. Whole PBMC RNA was extracted and levels of IFN γ and IL-4 mRNA were determined and normalized to 18S rRNA in relative quantification real-time PCR. 1-FAM is IFN γ mRNA from *EHV-1* with anti-CD28 co-stimulation, 2-FAM is IFN γ mRNA from PBMC with anti-CD28 only as negative control and 3-FAM is IFN γ mRNA from non-activated PBMC. 5-FAM is IL-4 mRNA from *EHV-1* with anti-CD28 co-stimulation, 6-FAM is IL-4 mRNA from PBMC with anti-CD28 only and 7-FAM is IL-4 mRNA from non-activated PBMC.

4.3.4.2 Tetanus toxoid stimulation

Tetanus toxoid (TT) is an antigen known to induce strong antibody (Th2) immune responses after vaccination. TT was used as another recall antigen for *in vitro* re-stimulation of equine PBMC. TT was first applied in different concentrations (2.00, 1.00 and 0.1 μ g/ml) with anti-CD28 (1 μ g/ml) for different durations of 6, 12, 18, 24 and 48 hours (data not shown).

Tetanus toxoid stimulation (0.1 μ g/ml) of horse PBMC induced high readouts that could also be best determined at 12 hours incubation and resulted in a significantly more pronounced level of mRNA expression of IL-4 compared to *EHV-1* (Fig. 29).

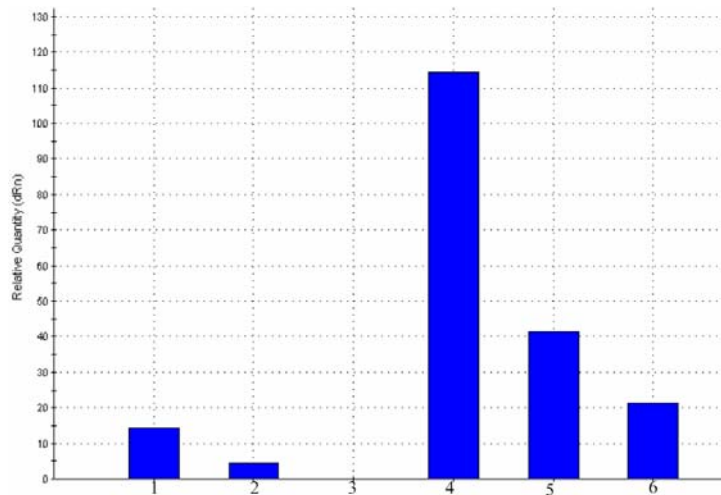


Fig. 29 Tetanus toxoid stimulation combined with anti-CD28 co-stimulation.

Horse PBMC were stimulated using TT (0.1 $\mu\text{g}/\text{ml}$) with co-stimulation of anti-CD28 (1 $\mu\text{g}/\text{ml}$) for 12 hours. Levels of mRNA expression of IL-4 and IFN γ were relatively quantified using real-time PCR.

Replicate (1) is IFN γ mRNA from TT with anti-CD28 co-stimulation, (2) is IFN γ mRNA from anti-CD28 only as negative control, (3) IFN γ mRNA from the nonactivated PBMC (calibrator), (4) IL-4 mRNA from TT with anti-CD28 co-stimulation, (5) IL-4 mRNA from anti-CD28 only as negative control and (6) IL-4 mRNA from the non-activated PBMC.

IFN γ and IL-4 mRNA expression readouts, obtained from *in vitro* stimulated horse PBMC with antigen-specific recall, suggested that maximal PBMC activation required the combined exposure to antigen recall (*EHV-1* or TT) and anti-CD28 co-stimulation. IFN γ and IL-4 expression levels were best measured after 12 hours stimulation.